



Delft University of Technology

## Glare-based control strategy for Venetian blinds in a mixed-use conference space with fully glazed facades

Theodoropoulou, Panagiota; Brembilla, Eleonora; Schipper, Roel; Louter, Christian

### DOI

[10.1016/j.jobe.2023.108181](https://doi.org/10.1016/j.jobe.2023.108181)

### Publication date

2024

### Document Version

Final published version

### Published in

Journal of Building Engineering

### Citation (APA)

Theodoropoulou, P., Brembilla, E., Schipper, R., & Louter, C. (2024). Glare-based control strategy for Venetian blinds in a mixed-use conference space with fully glazed facades. *Journal of Building Engineering*, 82, Article 108181. <https://doi.org/10.1016/j.jobe.2023.108181>

### Important note

To cite this publication, please use the final published version (if applicable).  
Please check the document version above.

### Copyright

Other than for strictly personal use, it is not permitted to download, forward or distribute the text or part of it, without the consent of the author(s) and/or copyright holder(s), unless the work is under an open content license such as Creative Commons.

### Takedown policy

Please contact us and provide details if you believe this document breaches copyrights.  
We will remove access to the work immediately and investigate your claim.



## Full length article

## Glare-based control strategy for Venetian blinds in a mixed-use conference space with fully glazed facades

Panagiota Theodoropoulou, Eleonora Brembilla<sup>\*</sup>, Roel Schipper, Christian Louter

Delft University of Technology, Delft, The Netherlands

## ARTICLE INFO

Dataset link: <https://github.com/pentheod/Optimized-control-strategy-CCC-TU-Delft>

## Keywords:

Living lab  
Fully glazed facades  
Control strategy  
Optimization  
Cylindrical illuminance

## ABSTRACT

Smart buildings are equipped with automated control systems that provide a comfortable indoor environment, aiming simultaneously at energy savings. Control systems for shading devices applied in practice are mostly driven by a rule-based approach, that is usually tested under simplified conditions and hence its effectiveness in complex real-life cases is questionable. The present study develops an optimized glare-based control strategy for Venetian blinds in a real-life open-space building with totally transparent facades. The research is based on the case study of the Co-Creation Center at the TU Delft campus, which can host three different types of events: presentations, meetings and workshops. The control strategy is developed within *Grasshopper*, a tool for parametric and optimization problems. Radial Basis Function Optimization (RBFOpt) is utilized for the computation of the optimal blinds' states. Within the developed control strategy, cylindrical illuminance ( $E_{cyl}$ ) is used as a glare index, giving the opportunity to evaluate its performance. Results show that the optimized algorithm can improve the existing visual conditions in the building by an average of 80% for all activity types, although it leads to an average increase of 7% of the time when electric lighting is needed, in comparison to the current rule-based control. Finally,  $E_{cyl}$  displayed an overall agreement of 92.5% with DGP-based glare assessments, proving that in spaces with multiple windows and uncertain occupants' view direction, a view-independent index can predict glare risks as well as a state-of-the-art view-dependent metric.

## 1. Introduction

Visual comfort depends on the amount and distribution of light in the indoor space. Allowing penetration of large amounts of daylight into the building can ensure sufficient indoor illuminance, limiting the need for electric lighting. In order to take advantage of the benefits of the incoming daylight, more and more buildings have been constructed with fully glazed facades over the last decades. However, concerns regarding visual and thermal discomfort that may occur due to excessive daylight, were quickly raised. On the one hand, stray light reaching users' eyes can provoke disability glare, resulting in a reduction of their visibility [1]. On the other hand, long exposure to excessive direct sunlight results in discomfort glare that may cause eye fatigue, headaches and dizziness [2]. In addition, during summer, large amounts of incoming solar energy lead to overheating of indoor spaces, and hence to higher cooling energy needs.

<sup>\*</sup> Corresponding author.

E-mail address: [E.Brembilla@tudelft.nl](mailto:E.Brembilla@tudelft.nl) (E. Brembilla).

<https://doi.org/10.1016/j.job.2023.108181>

Received 7 August 2023; Received in revised form 13 November 2023; Accepted 18 November 2023

Available online 22 November 2023

2352-7102/© 2023 The Authors. Published by Elsevier Ltd. This is an open access article under the CC BY license (<http://creativecommons.org/licenses/by/4.0/>).

To overcome those problems, but simultaneously maintain the benefits of daylight, multiple shading devices and complex fenestration systems have been developed [3]. Manual operation of blinds can be sufficient to ensure visual comfort based on the exact needs of the occupants, but usually at the cost of energy consumption. The gradual application of automatically controlled shading systems proved that they are a promising mechanism for the manipulation of the amount of admitted solar radiation, balancing visual comfort and energy demands at the same time [4].

Even though automatic shading systems have been thoroughly studied and applied to an increasing number of buildings over the last few years, their efficiency is still under investigation. This is because, state-of-the-art model-based algorithms achieve well-performing controls, but typically require long computational time, while traditional rule-based algorithms have low computational effort, but at the cost of their accuracy and effectiveness. The present study investigates an innovative glare-based control strategy of the shading system at the Co-Creation Center, a real-world building with an open-space floorplan, totally transparent facades and diverse occupancy patterns. The objective of this research can be defined as the development of a parametric model in *Grasshopper* that controls Venetian blinds using an optimization method, aiming at the maximization of visual comfort (prevention of glare and illuminance sufficiency), as well as the minimization of energy demands for electric lighting, in a multi-occupancy building with uncertain occupants' view directions and fully glazed facades.

### 1.1. Indices for glare assessment

Daylight Glare Probability (DGP) was proposed and evaluated by [5] as a glare metric highly correlated with users' response. DGP expresses the percentage of occupants that would be disturbed by discomfort glare for a given scene. DGP equation consists of two terms; the first one evaluates the level of illuminance perceived by the observer ( $E_{v,eye}$ ), while the second term represents the contrast ratio between the background average luminance and the glare source luminance. This fact makes DGP a robust index for glare assessment, as multiple studies have proven [6–8]. However, DGP is a view-dependent glare index, which implies that it needs a certain scene/view direction to assess glare risks.

Nevertheless, when assessing glare probability for spaces with many windows and various users' view directions, a metric that can assess glare sources for all orientations around an observer's position is needed. Furthermore, a real-time glare-based control strategy requires the fast computation of glare metrics, which is not feasible when employing image-dependent indices. These problems are resolved by cylindrical illuminance ( $E_{cyl}$ ), a metric that was initially proposed by [9]. Cylindrical illuminance ( $E_{cyl}$ ) is defined as the total luminous flux falling on the curved surface of a very small cylinder located at a specified point, divided by the curved surface area of the cylinder [10]. It represents the average of all vertical illuminances in all directions around a considered point.  $E_{cyl}$  can be used for view-independent glare assessments, as [11] proved that  $E_{cyl}$  can predict glare accurately and agree with DGP evaluations, after correlating the two indices.

### 1.2. Control strategies for shading systems

The most commonplace control strategy of a shading device is based on the calculation of outdoor illuminance or irradiance, either vertically on the façade or horizontally on the roof. This is a rule-based technique, implemented in most of the buildings that use smart control systems nowadays. Rule-based control strategies are usually combined with the cut-off angle method, the most typical manner to block direct solar beams passing through Venetian blinds. The widespread use of those control systems is due to thorough scientific investigation that proves their overall effectiveness and to their relatively easy implementation [3,12–14]. However, the existing studies mostly tackle simplified cases of side-lit rooms with a certain occupants' view direction [13,15–17]. As contemporary architecture tends to adopt open spaces for office and conference buildings, with windows towards various orientations, there is a need for a more complex evaluation of visual conditions in an indoor space, as well as more advanced techniques to operate shading devices. Hence, in lieu of geometrical controls of Venetian blinds and rule-based strategies, optimization methods for blinds' operation are lately under investigation [18–20]. Optimized control strategies use daylight and glare metrics as objectives, in order to find the optimal blinds' state that will ensure maximum visual comfort and minimum energy demand. Recently, [21] developed an Artificial Neural Network (ANN) to train an optimized control of Venetian blinds that automatically finds the optimal slat angle to balance visual comfort and energy savings. Although those studies have contributed significantly to the advancement of optimization algorithms for building physics, they have focused on rooms with certain orientations, facilitating the convergence of the algorithms and posing a challenge to the present research.

Generally, in optimized control strategies, the relation between the variables (blinds' states) and the objective (metrics) is not defined as a formula, and therefore the shape of the objective function is initially unknown. These cases can be tackled using black-box (or derivative-free) optimization methods, which do not require mathematical formulations of optimization problems. Model-based algorithms are a type of black-box optimization method that approximates the design space by constructing surrogate models of the implicit mathematical relations of the simulation-based models. Surrogate models demand shorter computational time than simulations, hence they can accelerate the optimization process. Every time the algorithm executes a new calculation, it improves the fitness landscape by gradually building and refining the surrogate model. This technique saves significant computational time, as the algorithm creates the fitness landscape and finds robust results with only a few iterations, without exhaustively repeating the time-intensive simulations. The high speed of convergence is important for sustainable design problems regarding daylighting, where a single simulation takes several minutes to complete. Due to their ability to model complex design spaces, Radial Basis Functions that follow a machine-learning approach are particularly suitable for architectural simulation-based problems, to construct the surrogate model [22,23].



Fig. 1. Co-Creation Center, TU Delft.

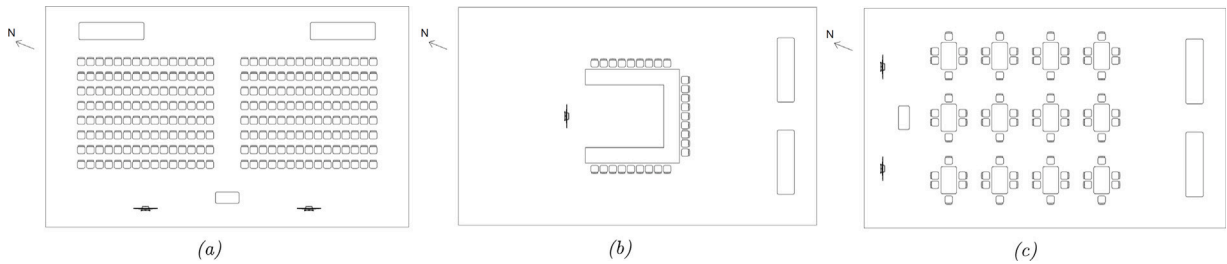


Fig. 2. Example of the space configuration for each of the occupancy modes: (a) presentation, (b) meeting, (c) workshop.

## 2. Methodology

### 2.1. Description of the case study building

The case study of the Co-Creation Center (CCC) serves as the basis of this research, therefore the developed control strategy directly concerns this particular building. The CCC is a conference space, located at the TU Delft campus in The Netherlands, constructed as a living lab for scientific research (Fig. 1). It is a single-story building with a rectangular open-space floorplan and four fully glazed facades that hosts three kinds of events: presentations, meetings and workshops (Fig. 2). The building is equipped with external Venetian blinds, that move simultaneously on each facade, but can potentially be individually operated.

The currently implemented blinds control strategy has two modes of operation. When the building is empty, the blinds' control tries to minimize the future energy needs for heating and cooling. On the other hand, when the building is occupied, the control system aims to limit glare risks. This study focuses on the occupied status. Currently, when the building hosts an event and when a facade is lit by direct radiation higher than  $100 \text{ W/m}^2$ , a sun-tracking control strategy is used to prevent solar beam penetration, meaning that the tilt of the blinds' lamellas is controlled in a way that always blocks direct sunlight (cut-off angle). In fact, the slat angle for all blinds on a facade is set to  $2^\circ$  more than the cut-off angle. When a facade receives mostly diffuse radiation (beam radiation less than  $70 \text{ W/m}^2$ ) and the blinds are already lowered, the slat angle is set to  $0^\circ$  to allow maximum outdoor view. If the blinds are down for at least 30 min and the direct radiation falls below  $50 \text{ W/m}^2$ , the blinds are raised. In order to make the rotation of the slat angles unnoticeable to the occupants, the control algorithm ensures that the tilt angle varies smoothly over time.

The current control system also operates electric lighting, by adjusting the lighting intensity of the luminaires to supplement daylight entry and reach the desired horizontal illuminance at desk level, which has a different target value depending on the activity. The current blinds' operation is the same for all occupancy modes, which are described below:

- **Presentation:** The orientation of the audience's view is predetermined, albeit not always the same. The desired illuminance at desk level is set to 300 lx, to ensure sufficient light for taking notes.
- **Meeting:** There is no specific orientation of the occupants. All of them sit around a desk. The desired illuminance at desk level is set to 500 lx.
- **Workshop:** There is no specific orientation of the occupants. Many desks are placed in the building and the users are distributed around them, working in groups. The desired illuminance at desk level is set to 750 lx.

**Table 1**  
Recommendations for daylight sufficiency [24].

Level of recommendation	Target illuminance (lx)
Minimum	300
Medium	500
High	750

**Table 2**  
Simulation ambient parameters for point-in-time simulations.

Parameter	Abbreviation	Used values
Ambient bounces	-ab	5
Ambient accuracy	-aa	0.2
Ambient resolution	-ar	64
Ambient divisions	-ad	4096
Ambient super-samples	-as	2048

**Table 3**  
Materials' optical properties used in the model.

Model element	Reflectance	Transmittance
<b>Building (Co-Creation Center)</b>		
Windows	–	0.68
Doors	–	0.80
Venetian blinds	0.04	–
Floor	0.30	–
Ceiling	0.30	–
Skylights	–	0.80
Overhang	0.01	–
<b>Context</b>		
Neighboring buildings	0.04–0.08	–
Ground	0.25	–
Canal	0.30	–
Plants	–	0.10 or 0.80
Climate tower	0.01	–

The above values of the desired horizontal illuminance are well aligned with the three levels of recommendation defined by [24]. Such standard states that, depending on the daylight needs for the activity taking place in the building, daylight design should achieve a target illuminance across 50% of the floor area for 50% of daylight hours, as presented in Table 1.

The building is equipped with a pyranometer placed on the roof, which records Global Horizontal Irradiance (GHI) every 5 min. [25] have indicated that the recorded irradiance data is reliable and therefore can be used for the simulation of the sky conditions. For the sky model, the GHI measurements are divided into Diffuse Horizontal Irradiance (DHI) and Direct Normal Irradiance (DNI) data, using the Skartveit splitting model [26].

## 2.2. Simulation model

A valid and accurate model of the Co-Creation Center and its surroundings is first created in *Grasshopper*. The latter is chosen as the basic software, because it combines three beneficial characteristics; (a) parametric modeling, (b) daylight simulations through the plug-in *Honeybee* and *Radiance* rtrace command, and (c) custom programming through Python.

The blinds of each window are operated by two variables: one for the vertical increment of the louvers and one for the angle of the slats. The slats can rotate between  $-30^\circ$  and  $72^\circ$  in steps of  $2^\circ$ , while the possible states of the blinds follow increments of 20%. To generate the 20% increment of blinds' movements, the distance between the slats is multiplied by a factor ranging from 0 to 1 in steps of 0.2. This constitutes the increment variable, with 0 representing blinds totally up and 1 representing blinds totally down.

In an attempt to represent realistic transmittance and reflectance values into the model, the materials' optical properties were measured in the field, under overcast conditions. However, after defining the simulation ambient parameters (Table 2) and validating the accuracy of the simulated sky model, the optical properties of some materials were modified in order to calibrate the model against outdoor and indoor illuminance sensor measurements. This choice was driven by the fact that many materials' characteristics were assumed, particularly for the outdoor scene elements. In Table 3 the final optical properties of the main model elements are listed.

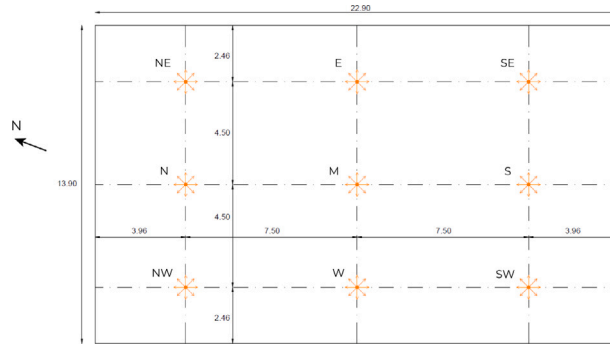


Fig. 3. Grid of viewpoints where DGP and  $E_{cyl}$  are calculated for the correlation of the two indices.

### 2.3. Correlation of $E_{cyl}$ with DGP

In the proposed control strategy, the metric employed for glare assessment is cylindrical illuminance ( $E_{cyl}$ ), because it is capable of imageless and view-independent glare evaluation with low computational cost. However, the fact that  $E_{cyl}$  does not introduce cut-off values for the distinction of the four glare classes (imperceptible, noticeable, disturbing, intolerable) entails the need for determination of those thresholds after correlating  $E_{cyl}$  with DGP. Since only imperceptible glare is allowed in the proposed control strategy, the DGP threshold of 0.35 is used in order to find the respective value for  $E_{cyl}$ .

For the correlation of the two indices, the approach of [11] is followed. For three test days with clear-sky conditions, various solar altitudes, and an hourly time resolution, the glare inside the CCC is assessed under two facades' conditions; blinds fully raised and blinds fully lowered with horizontal slats. Consequently, the glare evaluation is performed for six cases in total. The glare assessment is performed at a grid of nine viewpoints, evenly distributed in the space (Fig. 3). For each of those points, the vertical illuminance ( $E_v$ ) is calculated in eight directions at the height of 1.20 m (eye level of a seated person) and the average value is used to compute  $E_{cyl}$ . Finally, hemispherical fish-eye images are produced in each of the eight directions and DGP is calculated from them. For each of the six cases explained above, the highest DGP value of each point for each daylight hour is compared with the corresponding  $E_{cyl}$  value. In this manner, a large sample of 684 couples of values ( $E_{cyl}$ , DGP) is collected.

The next step is the arbitrary determination of a certain threshold for  $E_{cyl}$ . For this value, the following check is implemented for each couple of  $E_{cyl}$  and DGP values:

- True positive (TP): DGP > 0.35 and  $E_{cyl}$  over the chosen threshold.
- True negative (TN): DGP < 0.35 and  $E_{cyl}$  below the chosen threshold.
- False positive (FP): DGP < 0.35 and  $E_{cyl}$  over the chosen threshold.
- False negative (FN): DGP > 0.35 and  $E_{cyl}$  below the chosen threshold.

This check is repeated for multiple optional thresholds of  $E_{cyl}$ . The value providing the highest percentage of TP and TN results, and hence the highest agreement with DGP, is chosen as the final threshold. Eventually, it was found that the value of  $E_{cyl} = 1400$  lx is best employed in the proposed control strategy as the highest limit of imperceptible glare, because it shows a 93% agreement with the corresponding cut-off value of DGP.

### 2.4. Control strategy

The proposed control strategy of the blinds is steered by an optimization process, that leads to a theoretically ideal operation of the shading system. The optimization employed here is based on the Radial Basis Function Optimization (RBFOpt) algorithm, which can be performed by *Grasshopper's* component *Opossum* (OPTimizatiOn Solver with SURrogate Models). The priority of the optimized control system is the prevention of glare risks, which are evaluated by the maximum value of cylindrical illuminance ( $E_{cyl}$ ) among nine viewpoints (Fig. 3). The second aim of the developed control system is to provide sufficient amount of daylight in the space, in order to limit the need for electric lighting. The amount of daylight is quantified by the average horizontal illuminance on the workplace ( $E_{wp}$ ) calculated at a sensor grid 0.85 m above the floor, covering the whole floor area.

As illustrated in Fig. 4, based on the fixed inputs of the model for a specified time step and for a certain set of variables, the model calculates the average  $E_{wp}$  and the maximum  $E_{cyl}$  through point-in-time *Radiance* simulations. Based on these calculations, the optimization algorithm decides the optimal blinds' states that result in satisfactory values of  $E_{wp}$  and  $E_{cyl}$ . The optimization process is constrained by the limits of  $E_{wp}$  and  $E_{cyl}$ . In particular, to ensure an adequate quantity of light in the space,  $E_{wp}$  should be more than 300 lx, 500 lx and 750 lx for presentation, meeting and workshop respectively. At the same time, only imperceptible glare is allowed by employing the upper threshold of 1400 lx for  $E_{cyl}$ . The minimum limits of  $E_{wp}$  are the same as in the existing control strategy, following European Standard's recommendations. However, it should be noted that the deployed algorithm is stricter, and

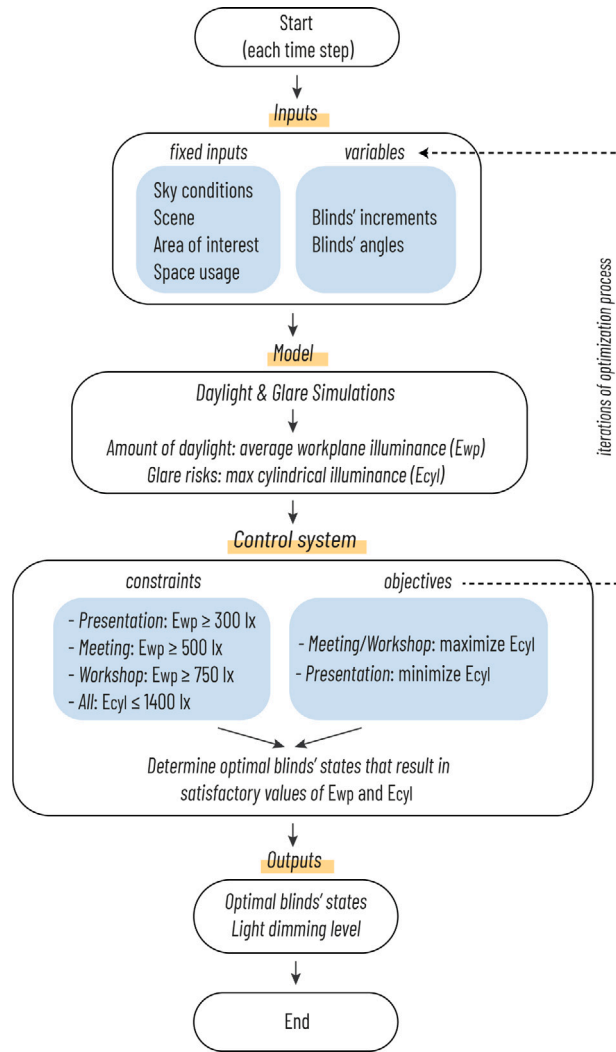


Fig. 4. Flowchart of the optimized control strategy.

thus more effective, in terms of daylight sufficiency, than the European Standard, because it aims to keep  $E_{wp}$  above the thresholds for 100% of the daylight hours and 100% of the floor area.

The fact that  $E_{wp}$  and  $E_{cyl}$  have overall similar trends as functions of the daylight quantity in the space, allows us to use only one of them as the objective of a Single-Objective Optimization (SOO) control algorithm. In the case of meetings and workshops, the aim is to prevent glare, while maximizing the amount of daylight so as to achieve low energy demands for electric lighting. The largest amount of daylight entry can be achieved only when  $E_{cyl}$  has a value close to 1400 lx, but still lower than this threshold. In this manner, noticeable glare is prevented, while the maximum possible  $E_{wp}$  is accomplished. On the contrary, for the presentation scenario, the light levels should be low, but sufficient to write down notes. The aim now is to minimize daylight entry until  $E_{wp}$  has a value close to 300 lx, but still higher than this limit. At the same time, a low  $E_{cyl}$  value should be accomplished ( $< 1400$  lx), ensuring minimal glare risks.

The optimization algorithm is described by the objective function of Eq. (1), where  $E_{cyl}$  is multiplied by a penalty factor. During workshops and meetings, the control system tries to maximize the objective function, whereas during presentations its minimization is targeted. The penalty is derived from the optimization constraints and is applied to enforce the algorithm to find values for  $E_{wp}$  and  $E_{cyl}$  within their limits.

$$\text{ObjectiveFunction} = \text{penalty} \times E_{cyl} \quad (1)$$

For each time step, the optimization runs through a certain number of iterations specified by the user (20 in this case), creating a loop in the process. The more the iterations, the higher the likelihood to find the optimal solution (blinds' states and corresponding values of  $E_{wp}$  and  $E_{cyl}$ ). Eventually, when the optimal blinds' states are determined, the algorithm decides the light dimming levels needed to supplement daylight, in case the average  $E_{wp}$  provided solely by daylight is not sufficient (Fig. 4).



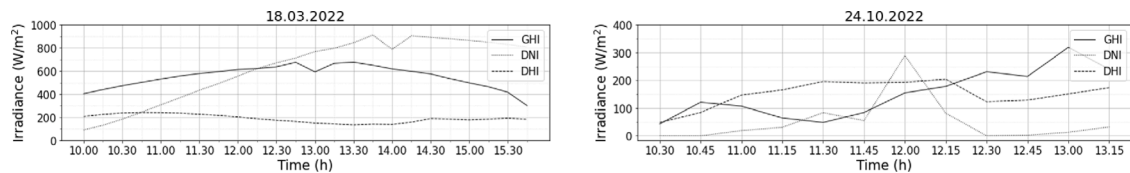


Fig. 5. Global Horizontal Irradiance measured by the CCC's roof sensor, as well as the respective Direct Normal and Diffuse Horizontal Irradiance calculated through the Skartveit model for the two test periods.

## 2.5. Validation of the control strategy

In order to validate the effectiveness of the proposed control model, its performance for the three activity modes is compared with the currently applied control system. The key performance indicators refer to:

- the amount of daylight in the space, expressed by the average  $E_{wp}$ ;
- the glare risks, evaluated by the maximum values of both  $E_{cyl}$  and DGP among the nine viewpoints, allowing to draw conclusions about the performance of  $E_{cyl}$  as a glare index;
- the quality of view towards the outdoors, calculated by the component “HB View Percent” and quantified as the average percentage of the occupants’ view that is not blocked by the blinds;
- the energy demands for electric lighting (in kW h);
- the solar heat gains (in kW h), giving insight into the solar energy performance of the proposed control strategy, although no further considerations on the energy demands for heating/cooling are made in this study.

The aforementioned data are obtained by performing the corresponding point-in-time simulations after importing the blinds’ states of each time step decided by the controllers. For the current control strategy, the blinds’ increments and angles are acquired from real logs, whereas for the optimized one, they are taken from the optimizations’ results.

The validation is done for two test days; the first one represents the worst-case scenario for glare risk (sunny sky, low solar altitude) and refers to 18.03.2022 between 10.00–16.00, while the second period represents variable weather conditions (cloudy and sunny sky) and refers to 24.10.2022 between 9.30–12.30. In Fig. 5, the GHI, DNI and DHI data are given for the two test periods. Both test periods belong to the heating season, meaning that solar heat gains are desired.

As the current blinds’ operation logs do not make a distinction between the three activity modes, there is no information about the exact type of activity that took place during those specific periods. Therefore, the results obtained by all the three optimized controls (for all three modes respectively) are compared with the corresponding outputs of the existing control, which is the same for the three cases. A time step of 15 min is chosen for the comparison of the two control models, using the louvers’ increments and tilt angles on the exact instant.

## 3. Results

In the following paragraphs, the results presenting the five performance indicators, obtained from the daylight, glare, view and energy analyses of the two control methods, for the two test days, are compared, based on the respective blinds’ configurations.

Figs. 6 and 7 illustrate the blinds’ states decided by the current control strategy and the optimized one for the workshop mode, over the two test periods. It is evident that, in both days, the current control results in a smoother operation of the blinds, while the optimized control leads to more erratic movements that might cause distraction to the occupants during a session. As expected, during the second day, with variable weather conditions, the developed control results in more abrupt blinds’ movements than during the first test day. Nevertheless, thanks to the 20% increment step of the optimized control, there are intervals (e.g. 12.00–14.00 in Fig. 6) where the shades are lowered or raised to the next increment step, facilitating the provision of visual comfort with small movements and hence without causing much nuisance to the users.

Figs. 8 and 9 show the overall performance of the control strategies during the two test periods, in terms of daylight sufficiency, glare risks and view quality. As regards the amount of daylight in the indoor space, the existing control system generally results in high  $E_{wp}$  values most of the time than the three activity modes of the optimized control, meaning that more light is allowed to pass through the facades (Figs. 8(a), 9(a)). This is desired when a meeting or a workshop takes place, but it is unwanted during a presentation when the occupants’ focus should be on the projection screen. On the other hand, the optimized control for the presentation mode generally manages to minimize  $E_{wp}$  close to the target value of 300 lx, usually without creating the need for electric lighting. In the case of a meeting and workshop, the maximum limit of  $E_{cyl}$  makes the developed control stricter, letting less daylight enter the space than the current control, but usually enough to meet the minimum limits. Only for a few time steps, the minimum thresholds of 500 lx and 750 lx are not reached, but this is reasonable as energy minimization was not the priority of the developed control strategy. It is worth noticing that, at the beginning of the session on 24.10.2022 (Fig. 9(a)), when the global, direct and diffuse irradiance is very low, neither of the two control strategies manages to keep  $E_{wp}$  above the minimum thresholds of the meeting and workshop, although they both have totally raised blinds.



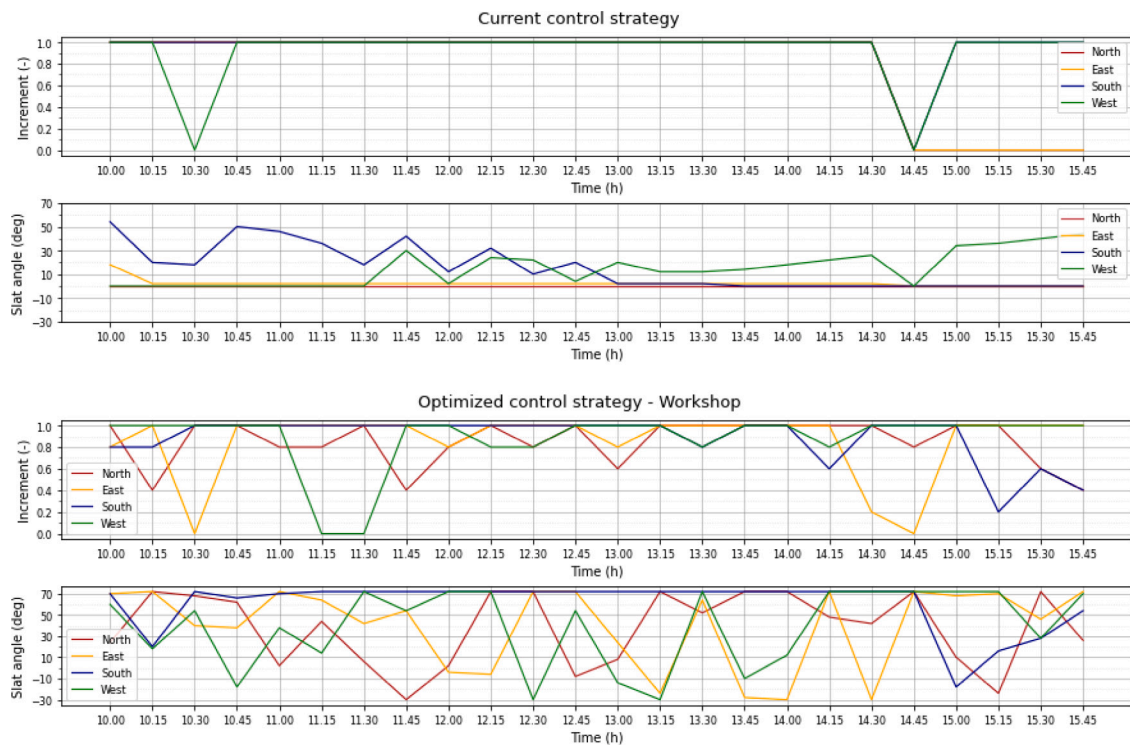


Fig. 6. Blinds' states decided by the current control and the optimized one for the workshop mode over the test period on 18.03.2022.

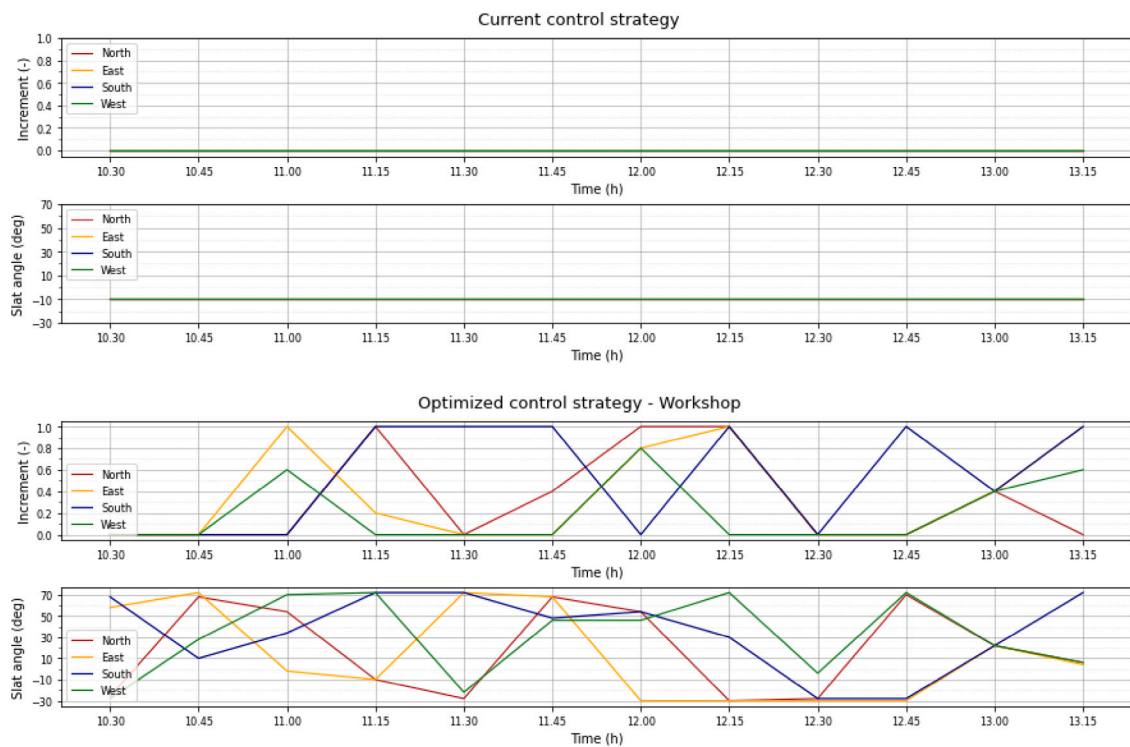


Fig. 7. Blinds' states decided by the current control and the optimized one for the workshop mode over the test period on 24.10.2022.

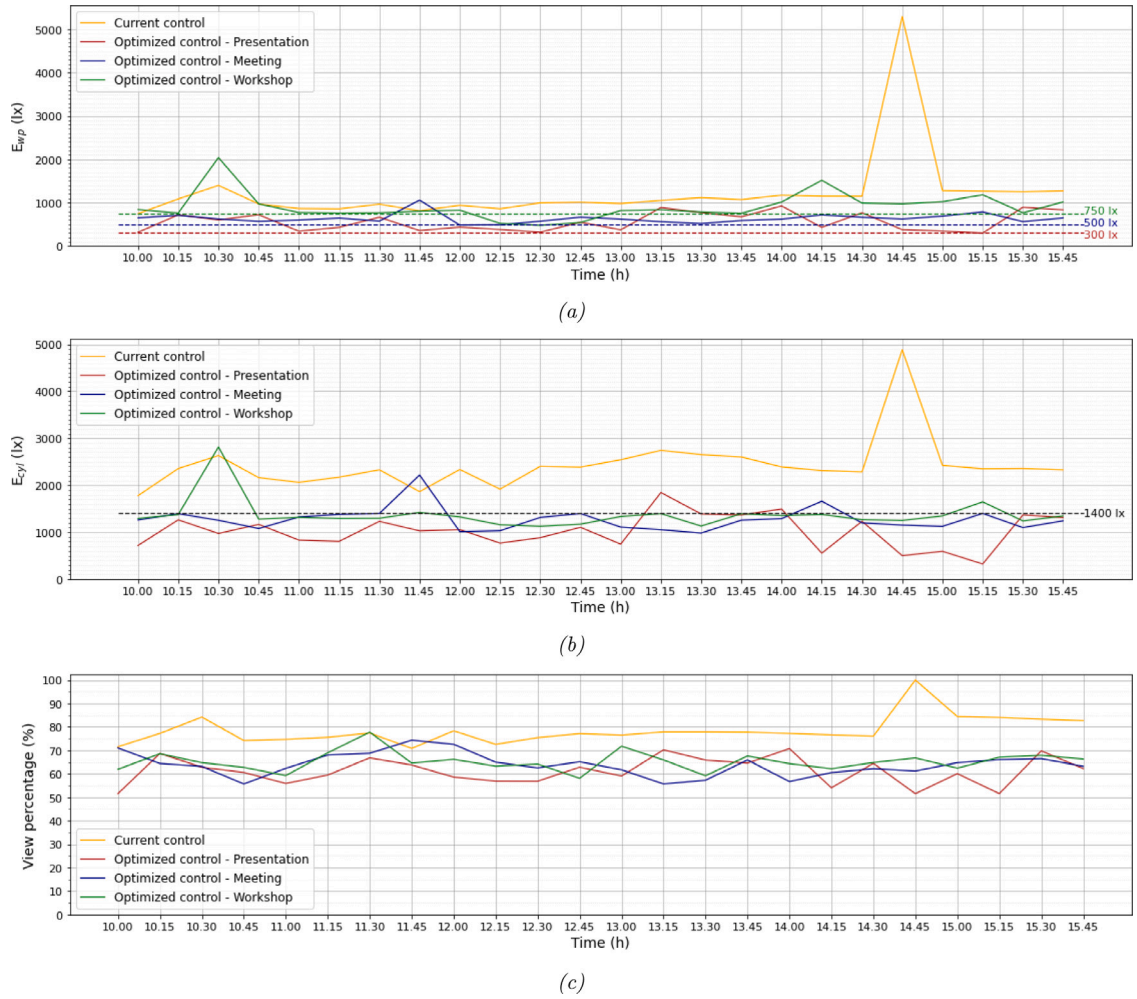


Fig. 8. (a) Workplane illuminance, (b) cylindrical illuminance and (c) view percentage for all control strategies throughout the test period on 18.03.2022.

Figs. 8(b) and 9(b) clearly show that the high daylight admission of the currently implemented control leads to high glare risks in both test periods. On the contrary, the developed control system guarantees zero glare risks most of the time for all activity scenarios, except for only a few time steps of the sunny test period where  $E_{cyl}$  exceeds 1400 lx (Fig. 8(b)). For those instances, the algorithm shows some difficulty to converge to a non-glare solution, probably due to incoming direct or diffuse daylight passing through unshaded western and eastern glass doors.

As regards the view quality, Figs. 8(c) and 9(c) demonstrate the average percentage of the occupants' view that is not blocked by the blinds throughout the event. The graphs prove that the lower amount of admitted daylight in the optimized control does not compromise essentially the occupants' view to the outside, although it is clear that the current control provides better view quality, especially on the second analyzed day, when the blinds are constantly up. The higher amount of daylight entry during the meeting and workshop modes of the optimized control slightly increases the view quality in comparison to the presentation mode, although no large differences are observed. It is worth noticing that, with the optimized algorithm, the average view percentage displays higher fluctuations, mainly under variable weather conditions.

Figs. 10 and 11 demonstrate in detail the glare risks distributed over the space during the sunny test interval. Every rectangle represents the floor plan, divided into nine smaller rectangles that outline the nine viewpoints where glare is assessed, as indicated in Fig. 3. Every viewpoint is evaluated based on its maximum DGP value among eight view directions and its  $E_{cyl}$  (average of vertical illuminances among the eight directions). As expected, when the blinds are totally raised during the sunny day, the two metrics agree by 100% that there is constantly excessive daylight in the space, causing glare to all positions. With the currently implemented control strategy, only a small improvement is achieved in glare risks over the sunny test period. During the second day, the current control, that maintains the blinds constantly raised, results in glare risks when diffuse irradiance exceeds  $120 \text{ W/m}^2$  or direct sunlight enters the space.

On the contrary, for the vast majority of the time steps of both periods, the optimized control strategy successfully prevents glare, especially based on the  $E_{cyl}$  glare assessment that steers the optimization. It is noticeable that the DGP-based assessment

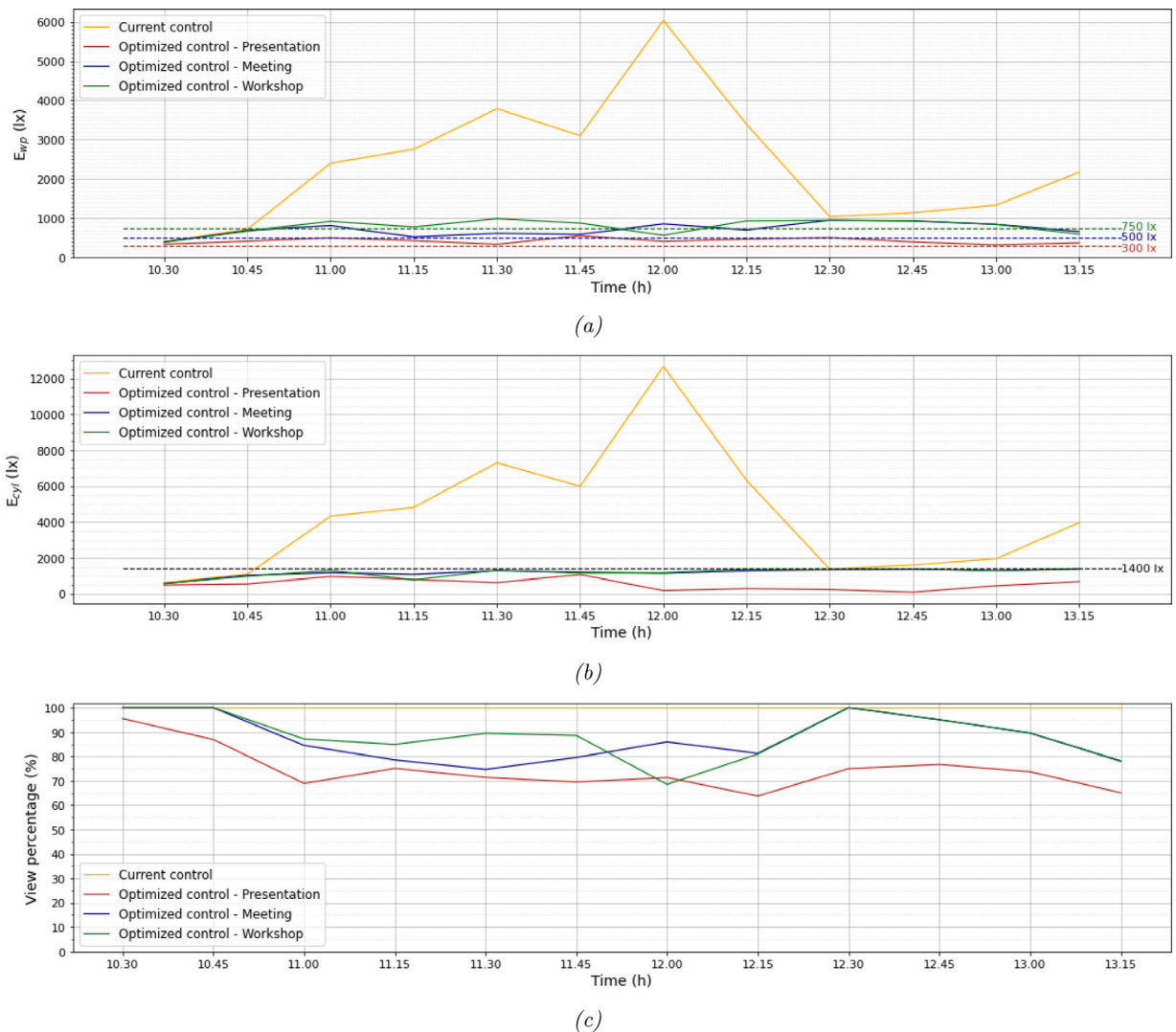


Fig. 9. (a) Workplane illuminance, (b) cylindrical illuminance and (c) view percentage for all control strategies throughout the test period on 24.10.2022.

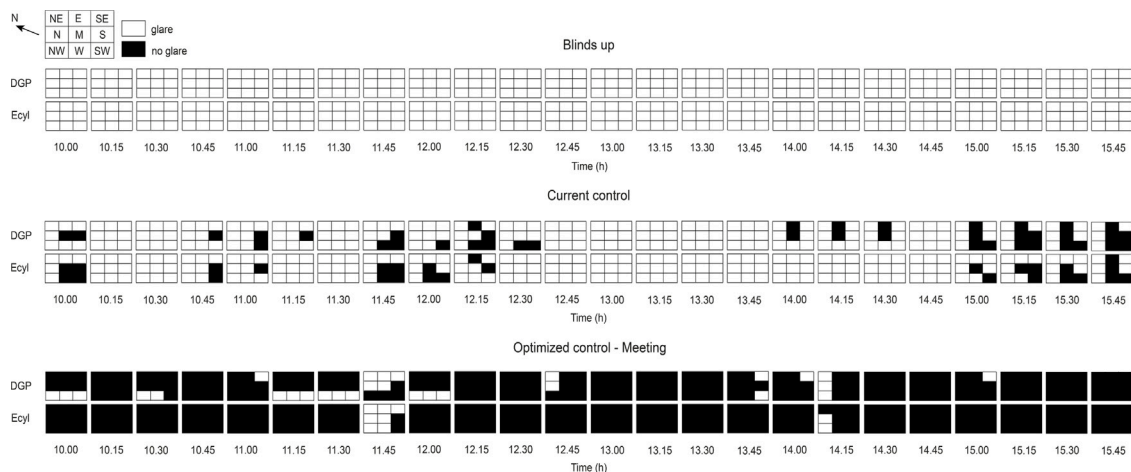
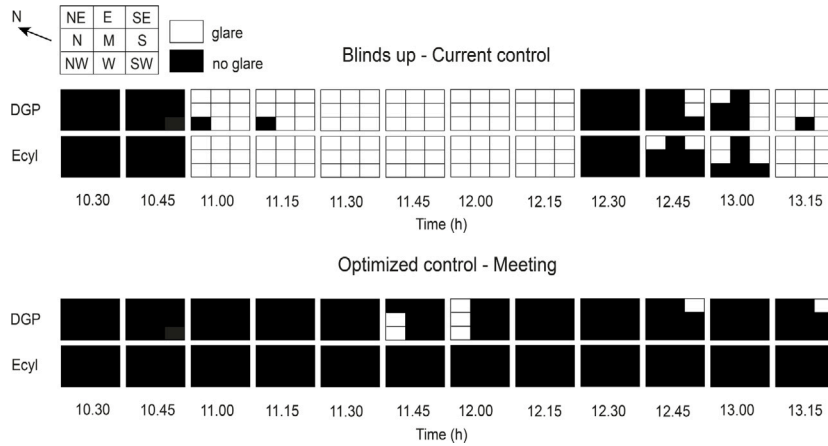
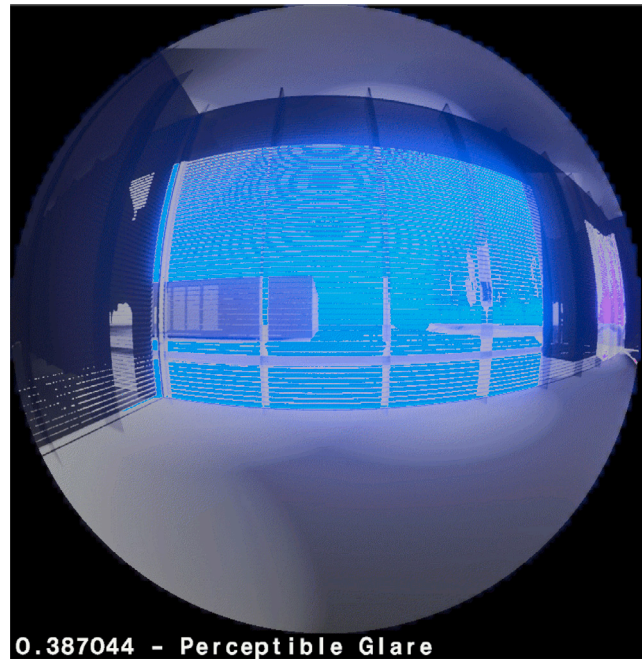


Fig. 10. Demonstration of glare and no glare positions over the test period on 18.03.2022 for totally raised blinds, the current control and the optimized one for the meeting mode.



**Fig. 11.** Demonstration of glare and no glare positions over the test period on 24.10.2022 for totally raised blinds, the current control and the optimized one for the meeting mode.



**Fig. 12.** Example of glare due to luminance contrast at the southern view direction, based on the DGP-based assessment (meeting mode, at 14.00 on 18.03.2022).

slightly overestimates the glare risks. The reason behind this is that  $E_{cyl}$  evaluates glare based only on the amount of light perceived by the occupant's eyes, whereas DGP additionally considers the contrast effect between the background and the glare source's luminance. High contrast effects occur due to the darker indoor conditions and the bright daylight that penetrates unshaded parts of the facades or through the louvers. An example of such a condition can be seen in Fig. 12, which shows the HDR image resulting from the DGP-based glare assessment in the southern view direction of the South-East viewpoint, at 14.00 on 18.03.2022. Based on  $E_{cyl}$ , there is no glare risk, whereas based on DGP, the viewpoint experiences glare towards that direction due to the contrast effect explained above. The average percentages of glare reduction (in comparison to the blinds-up situation) and the agreement between  $E_{cyl}$  - DGP for all cases, over the two test periods, are summarized in Table 4.

Fig. 13 presents the lighting energy demands for each activity scenario under the current and the optimized control, over the two analyzed intervals. The large amounts of incoming daylight allowed by the current system during the sunny test period results in almost zero lighting energy needs for all activities. However, the low illuminance levels at some time steps of the second test period do not suffice to meet the minimum requirements of  $E_{wp}$  for the meeting and workshop and hence electric lighting is needed. On the



**Table 4**

Improvement of glare conditions compared to totally raised blinds based on  $E_{cyl}$  and DGP, and agreement between the two glare indices for the different blinds' operations over the two test periods.

	Blinds up	Current control	Optimized control Presentation	Optimized control Meeting	Optimized control Workshop
Improvement based on DGP (%)	–	4.7	96	91	89
Improvement based on $E_{cyl}$ (%)	–	3.3	99	99	99
$E_{cyl}$ - DGP agreement (%)	97	91	95	92	90

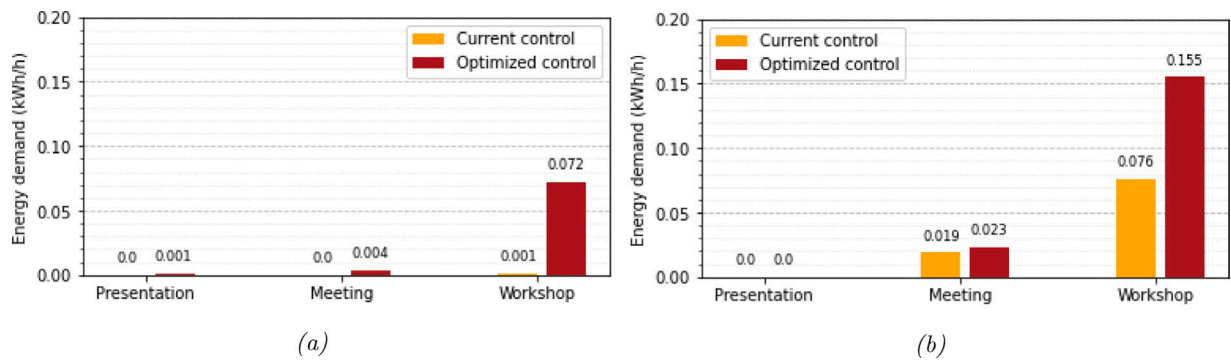


Fig. 13. (a) Energy demands for electric lighting resulting from the two control systems for the three activity scenarios during the test periods on (a) 18.03.2022 and (b) 24.10.2022.

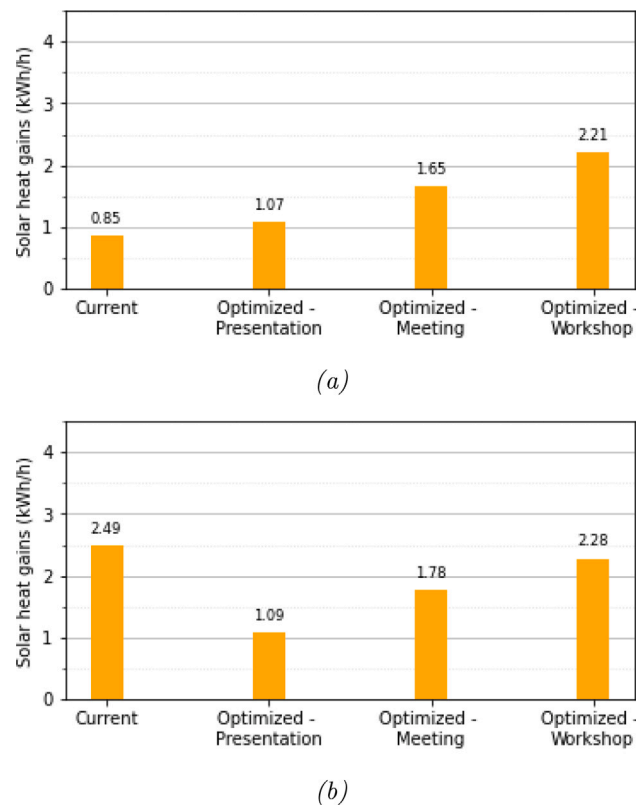


Fig. 14. Solar heat gains for the current control and the optimized one for the three activity modes during the test periods on (a) 18.03.2022 and (b) 24.10.2022.

other hand, the optimized control usually leads to higher energy consumption, with the workshop demanding a more considerable energy amount. This is reasonable, as the strict  $E_{cyl}$  threshold of 1400 lx, makes the optimization convergence to high  $E_{wp}$  values (>750 lx) difficult.

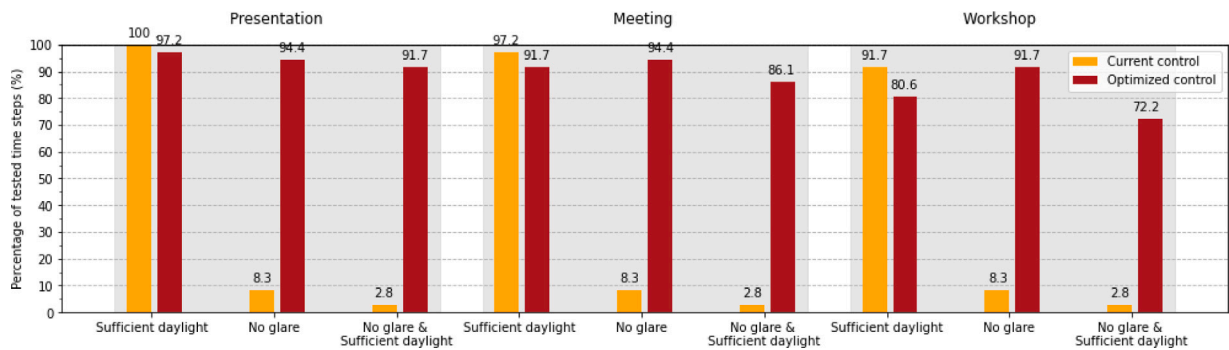


Fig. 15. Percentage of time steps of the two test periods where sufficient daylight, zero glare risks, and both of them are noted for each of the activity scenarios. Here, the percentages refer to  $E_{cyl}$ -based glare assessment.

The solar heat gains resulting from the four controls over the two test periods are demonstrated in Fig. 14. It is evident that, in spite of the different blinds' operations between the two analyzed periods, the optimized control results in fairly constant incoming solar radiation for all activity types, as the blinds' states are controlled in a way to constantly maintain visual comfort, meeting the requirements for  $E_{wp}$  and  $E_{cyl}$ .

Overall, the daylight performance of the developed control algorithm is satisfactory, providing visual comfort most of the time for all viewpoints. Fig. 15 presents the percentage of the time steps of the two test periods where sufficient daylight, zero glare risks and both of them occur for the three activity modes under the two control systems. In terms of daylight adequacy, the current system slightly outperforms the proposed one, but at the cost of glare risks. On the contrary, the optimized algorithm keeps a balance between daylight sufficiency and glare prevention, reducing the time steps with glare risks by an average of 85% in all cases, but increasing the time steps where electric lighting is needed by only 7%, in comparison to the existing control. In total, ideal visual conditions with adequate daylight and zero glare over the space, are achieved at a much higher average percentage of the tested time (80%) than in the current control, with the workshop being the most complex case for the algorithm to converge. Finally, the glare assessments by DGP and  $E_{cyl}$  were overall similar, reaching a mean agreement percentage of 92.5%. This proves that the *a priori* correlation of the two indices was performed thoroughly and successfully.

#### 4. Discussion

The developed control strategy for the automatic operation of Venetian blinds was proved generally successful in the complex case of the Co-Creation Center. However, prioritizing glare led to stricter results in terms of daylight quantity in the space and therefore the energy demands for electric lighting were slightly higher than in the current control. The fact that the developed algorithm worked effectively in the mixed-use case-study building, suggests that it can be trustfully implemented in buildings with multiple glare sources that host presentations, meetings or workshops and generally have uncertain occupants' view directions. The chosen 20% resolution of blinds' increments was found beneficial for the provision of visual comfort and the smoothness of blinds' operations.

In this research, the blinds' movement is performed simultaneously on each facade, as a more independent operation would result in dramatically high computational effort. However, even in the simplest blinds' operation, the runtime of 1 h to obtain satisfactory results is still prohibitive for a real-time controller of a shading system. The long runtime was due to the noticeably time-consuming ray-tracing analyses performed by *Grasshopper* using the *rtrace* command for the point-in-time simulations of the optimization. At the same time, although RBOpt was a successful optimization tool for fast convergence, its component in *Grasshopper* (*Opossum*) is not suitable for iterative processes, because it needs manual commencement of the optimization process for each time step. Improving the overall performance of the parametric software by its developers is a necessity, as this would facilitate the development of a control strategy at least in the design stage. Currently, aiming to drastically reduce the runtime, choosing another programming language (e.g. Python, Matlab, C++) would help execute faster the optimization iterations. Additionally, using the 3- or 5-phase methods (either in *Grasshopper* or in another programming language), would save computational effort, as the light transport in the exterior could be calculated only once throughout the optimization iterations for each time step [27].

The outputs of the optimized algorithm were obtained after 20 iterations. This means that the results were not the deterministically optimal ones (global minimum or maximum), but, in most of the cases, they converged and were found to be acceptable. This guarantees that after re-performing the optimizations, they would generally produce similar results. More iterations might provide a higher probability that the actual best solution is reached, but at the cost of computational time. Of course, reaching the optimal solution does not necessarily imply that the algorithm would converge to a satisfactory result, as this depends on the conditions of the specific time step. For a few time steps, the control algorithm did not achieve a satisfactory solution. This means that more iterations would be needed to facilitate the convergence to a good result, although this is not guaranteed. The validation process revealed that unsuccessful optimizations that resulted in glare or insufficient daylight, occurred with a small average percentage

**Table 5**  
Proposed control algorithm per building use.

Building use	Algorithm method
Presentations	Minimize $E_{cyl}$ until $E_{wsp} > 300 \text{ lx}$
Meetings	Maximize $E_{cyl}$ until $E_{cyl} < E_{cyl,max}^a$
Workshops	Maximize $E_{cyl}$ until $E_{cyl} < E_{cyl,max}^a$

<sup>a</sup> After correlating  $E_{cyl}$  with DGP for a specific space.

of 16% for the three activity modes. This shows that the algorithm is reliable with a high possibility to converge to a satisfactory solution.

In terms of glare assessment,  $E_{cyl}$  was proven a generally reliable index for the identification of glare risks due to large daylight amounts in the space. However, when the room is mostly dim and solar beams or daylight pass through the louvers, high contrast effects may occur, which are not taken into account by  $E_{cyl}$ . Although this constitutes a limitation for the universal use of  $E_{cyl}$  as a glare index, its application in complex cases with multiple glare sources (i.e. windows) is encouraged since it can resemble DGP results most of the time, with lower computational cost. Future research should investigate the correlation between those metrics and actual occupants' satisfaction by means of field experiments.

In general, the automatically controlled shading systems implemented in practice aim at the provision of visual comfort, neglecting the energy performance of the buildings in terms of heating and cooling. Although research has been implemented on the development of automatic shading controllers for both daylight and energy, multiple studies have shown that balancing the daylight and energy performance of a building, by utilizing one shading system, is a challenging task [28–30]. Previous studies proved that it is difficult to improve both visual comfort and energy consumption simultaneously; the level of improvement in the various performance indicators depends on their order of priority. These conclusions are supported by the findings of the present study, which showed that the priority of the control to maintain visual comfort when the building is occupied does not allow for large differentiation of the admitted solar radiation depending on the weather conditions. This observation raises concerns about the solar heat gains during the cooling season; as the system operates the blinds always the same way (keeping  $E_{cyl}$  and  $E_{wsp}$  within the desired limits), regardless of the sky conditions, the admitted solar radiation will probably display a constant trend over the year. This assumption should be confirmed with additional analyses in the cooling season.

The fact that glare-based control systems aim to constantly maintain the same desired visual conditions in the building on a yearly basis, while energy-based controls should adjust their behavior depending on the season, creates an incompatibility between them. In the case study building, this justifies the decision to utilize two modes of shading control dependent on the occupancy status, for daylight and thermal performance separately, following a similar approach to [31]. An alternative way to balance daylight entry and heating/cooling demands at the same time is to utilize two shading devices in the same control system. For instance, outdoor Venetian blinds could be operated only for constant solar heat gains regulation, while indoor roller blinds could be applied to provide visual comfort during occupied hours.

## 5. Conclusion

This research supported the development of a glare-based control strategy for the automatic operation of Venetian blinds in a space with multiple daylight sources (i.e. windows) and variable occupancy cases (presentations, meetings, workshops). The deployed control strategy was steered by a black-box optimization process based on RBFOpt. Within the scope of this research, the performance of cylindrical illuminance ( $E_{cyl}$ ) as a glare index was additionally assessed. The study proved the effectiveness of the developed control algorithm, which indicates that it can be applied in practice in buildings with multiple windows that host presentations, meetings or workshops and generally have uncertain occupancy patterns (Table 5).

Overall, the developed optimized control of the blinds was found to outperform the current rule-based one in terms of occupants' visual comfort. In fact, the algorithm achieved providing ideal visual conditions (zero glare risks and daylight sufficiency) for the majority of the tested time steps, specifically for 92%, 86% and 72% of the analyzed time for the presentation, meeting and workshop modes respectively. Although the optimized control reduced the current glare risks by an average of 80%, its priority to prevent glare led to an average increase of 7% in the time steps where electric lighting was needed, in comparison to the current control. As regards glare assessment,  $E_{cyl}$  displayed an overall agreement of 92.5% with DGP, proving that their correlation was done successfully. This indicates that in complex spaces with many windows and uncertain occupants' view directions, it is beneficial to use a view-independent index, as it can predict glare risks adequately well, after being carefully correlated with another reliable view-dependent index.

## Supplementary data

More information about the research project and detailed results from the analyses are presented in the Master thesis “Optimized control strategy for Venetian blinds in an event space with fully glazed facades: The case study of the Co-Creation Center”, at <https://repository.tudelft.nl>. The Python script of the control strategy's algorithm can be found in the GitHub repository: <https://github.com/pentheod/Optimized-control-strategy-CCC-TU-Delft>



## CRediT authorship contribution statement

**Panagiota Theodoropoulou:** Methodology, Software, Validation, Writing – original draft. **Eleonora Brembilla:** Conceptualization, Writing – review & editing, Supervision. **Roel Schipper:** Supervision. **Christian Louter:** Writing – review & editing, Supervision.

## Declaration of competing interest

The authors declare the following financial interests/personal relationships which may be considered as potential competing interests: Eleonora Brembilla reports financial support was provided by Netherlands Enterprise Agency. Panagiota Theodoropoulou reports financial support was provided by Alexander S Onassis Public Benefit Foundation.

## Data availability

The Python script of the control strategy's algorithm can be found in the GitHub repository: <https://github.com/pentheod/Optimized-control-strategy-CCC-TU-Delft>.

## Acknowledgments

Dr. Brembilla acknowledges the assistance offered by Wouter Beck, as well as the support from the Converge project (RVO TKI Urban Energy TEUE318008) and all the partners involved (Stichting The Green Village, Priva BV, Orange Climate BV, Hunter Douglas). Ir. Theodoropoulou was supported by the Onassis Foundation - Scholarship ID: F ZR 018-1/2021-2022.

## References

- [1] J.J. Vos, Disability Glare: a State of the Art Report, Commission Int. de l' Eclairage, 1984, pp. 39–53.
- [2] W.K. Osterhaus, Discomfort glare assessment and prevention for daylight applications in office environments, in: *Solar Energy*, 79, (2) 2005, pp. 140–158.
- [3] M. Konstantoglou, A. Tsangrassoulis, Dynamic operation of daylighting and shading systems: A literature review, *Renew. Sustain. Energy Rev.* 60 (2016) 268–283.
- [4] M.V. Nielsen, S. Svendsen, L.B. Jensen, Quantifying the potential of automated dynamic solar shading in office buildings through integrated simulations of energy and daylight, *Sol. Energy* 85 (5) (2011) 757–768.
- [5] J. Wienold, J. Christoffersen, Evaluation methods and development of a new glare prediction model for daylight environments with the use of CCD cameras, *Energy Build.* 38 (7) (2006) 743–757.
- [6] J.A. Jakubiec, C.F. Reinhart, The 'adaptive zone'-A concept for assessing discomfort glare throughout daylight spaces, *Light. Res. Technol.* 44 (2) (2012) 149–170.
- [7] J. Suk, M. Schiler, Investigation of Evalglare software, daylight glare probability and high dynamic range imaging for daylight glare analysis, *Light. Res. Technol.* 45 (4) (2013) 450–463.
- [8] J. Wienold, T. Iwata, M. Sarey Khanie, E. Erell, E. Kaftan, R.G. Rodriguez, J.A. Yamin Garretton, T. Tzempelikos, I. Konstantzos, J. Christoffersen, T.E. Kuhn, C. Pierson, M. Andersen, Cross-validation and robustness of daylight glare metrics, *Light. Res. Technol.* 51 (7) (2019) 983–1013.
- [9] H. Hewitt, D.J. Bridgers, R.H. Simons, Lighting and the environment: Some studies in appraisal and design, in: *Transactions of the Illuminating Engineering Society*, London, 1965.
- [10] J.T. Duff, Code for lighting: The impact on design and commissioning, *Sdar\* J. Sustain. Des. Appl. Res.* 1 (2) (2012).
- [11] S. Torres, V.R. Lo Verso, Comparative analysis of simplified daylight glare methods and proposal of a new method based on the cylindrical illuminance, *Energy Procedia* 78 (2015) 699–704.
- [12] A. Tzempelikos, H. Shen, Comparative control strategies for roller shades with respect to daylighting and energy performance, *Build. Environ.* 67 (2013) 179–192.
- [13] Y.C. Chan, A. Tzempelikos, Efficient venetian blind control strategies considering daylight utilization and glare protection, *Sol. Energy* 98 (PC) (2013) 241–254.
- [14] S. Zhang, D. Birru, An open-loop venetian blind control to avoid direct sunlight and enhance daylight utilization, *Sol. Energy* 86 (3) (2012) 860–866.
- [15] S. Vanage, H. Dong, K. Cetin, Visual comfort and energy use reduction comparison for different shading and lighting control strategies in a small office building, *Sol. Energy* (ISSN: 0038-092X) 265 (2023) 112086, <http://dx.doi.org/10.1016/j.solener.2023.112086>.
- [16] A. Eltaweel, Y. Su, Controlling venetian blinds based on parametric design; via implementing Grasshopper's plugins: A case study of an office building in Cairo, *Energy Build.* 139 (2017) 31–43.
- [17] I. Konstantzos, A. Tzempelikos, Y.C. Chan, Experimental and simulation analysis of daylight glare probability in offices with dynamic window shades, *Build. Environ.* 87 (2015) 244–254.
- [18] A. Mahdavi, Predictive simulation-based lighting and shading systems control in buildings, *Build. Simul.* 1 (1) (2008) 25–35.
- [19] V. Čongradac, M. Prica, M. Paspalj, D. Bojanić, D. Čapko, Algorithm for blinds control based on the optimization of blind tilt angle using a genetic algorithm and fuzzy logic, *Sol. Energy* 86 (9) (2012) 2762–2770.
- [20] Y. Wang, Y. Weibin, Q. Wang, Multi-objective parametric optimization of the composite external shading for the classroom based on lighting, energy consumption, and visual comfort, *Energy Build.* 275 (2022).
- [21] F. Nicoletti, D. Kaliakatos, M. Parise, Optimizing the control of venetian blinds with artificial neural networks to achieve energy savings and visual comfort, *Energy Build.* (ISSN: 0378-7788) 294 (2023) 113279, <http://dx.doi.org/10.1016/j.enbuild.2023.113279>.
- [22] T. Wortmann, Model-based optimization for architectural design: Optimizing daylight and glare in Grasshopper, *Technol. Archit. Des.* 1 (2) (2017) 176–185.
- [23] A. Forrester, A. Sobester, A. Keane, *Engineering Design Via Surrogate Modelling: A Practical Guide*, Wiley, J., Chichester, UK, 2008.
- [24] NEN-EN 17037, Natural Lighting of Buildings – Assessment of Daylight in Buildings, CEN, CEN (European Committee for Standardization), 2018.
- [25] P. Van den Engel, R. Bokel, E. Brembilla, L. de Araujo Passos, P. Luscuere, CONVERGE: Low energy with active passiveness in a transparent highly occupied building, in: *REHVA 14th HVAC World Congress*, Vol. 111, 2022.
- [26] A. Skartveit, J.A. Olseth, A model for the diffuse fraction of hourly global radiation, *Sol. Energy* 38 (4) (1987) 271–274.

- [27] E. Brembilla, T. Wang, P. Theodoropoulou, W. Beck, Evaluation of blinds control techniques for daylight and visual comfort in complex real-world conditions, in: Building Simulation Conference, International Building Performance Simulation Association (IBPSA), 2023.
- [28] D. Lee, Y.H. Cho, J.H. Jo, Assessment of control strategy of adaptive façades for heating, cooling, lighting energy conservation and glare prevention, *Energy Build.* 235 (2021).
- [29] D.M. Le, D.Y. Park, J. Baek, P. Karunyasopon, S. Chang, Multi-criteria decision making for adaptive façade optimal design in varied climates: Energy, daylight, occupants' comfort, and outdoor view analysis, *Build. Environ.* 223 (2022).
- [30] J. Yao, An investigation into the impact of movable solar shades on energy, indoor thermal and visual comfort improvements, *Build. Environ.* 71 (2014) 24–32.
- [31] A. Guillemin, N. Morel, An innovative lighting controller integrated in a self-adaptive building control system, *Energy Build.* (2001)